

# Pipeline Parallelism with Controllable Memory

Penghui Qi<sup>\*12</sup>, Xinyi Wan<sup>\*1</sup>, Nyamdavaa Amar<sup>†2</sup>, Min Lin<sup>1</sup>

<sup>1</sup>Sea AI Lab

<sup>2</sup>National University of Singapore

{qiph, wanxy, linmin}@sea.com amara@u.nus.edu

## Abstract

Pipeline parallelism has been widely explored, but most existing schedules lack a systematic methodology. In this paper, we propose a framework to decompose pipeline schedules as repeating a building block and we show that the lifespan of the building block decides the peak activation memory of the pipeline schedule. Guided by the observations, we find that almost all existing pipeline schedules, to the best of our knowledge, are memory inefficient. To address this, we introduce a family of memory efficient building blocks with controllable activation memory, which can reduce the peak activation memory to 1/2 of 1F1B without sacrificing efficiency, and even to 1/3 with comparable throughput. We can also achieve almost zero pipeline bubbles while maintaining the same activation memory as 1F1B. Our evaluations demonstrate that in pure pipeline parallelism settings, our methods outperform 1F1B by from 7% to 55% in terms of throughput. When employing a grid search over hybrid parallelism hyperparameters in practical scenarios, our proposed methods demonstrate a 16% throughput improvement over the 1F1B baseline for large language models.

## 1 Introduction

Distributed model training has attracted a lot of attention in recent years, especially after the boom of large language models [Brown et al., 2020]. As the model size becomes larger and larger, data parallelism (DP) [Goyal et al., 2017] is no longer capable to hold all the parameters in a single device. Under this background, model parallelism [Harlap et al., 2018, Huang et al., 2019, Shoeybi et al., 2019, Zheng et al., 2022] is proposed to partition parameters into a set of devices to address the memory constraint. tensor parallelism (TP) [Shoeybi et al., 2019] is a commonly used model parallel strategy, which partitions weight parameters into several devices and performs matrix multiplication separately. A well-known shortcoming of TP is that, it requires a lot of communication volume, which makes it inefficient when bandwidth becomes the bottleneck Narayanan et al. [2021]. In such situations, pipeline parallelism [Harlap et al., 2018, Huang et al., 2019], which is another model parallel strategy, shows its advantage in low communication cost. The core idea of pipeline parallelism is to split the entire model into several stages, which can be processed by several devices in a streaming way. In a typical large-scale training scenarios such as Narayanan et al. [2021], TP is generally used within one compute node, and PP is used to scale up across nodes.

Although PP has been widely adopted and developed, it suffers from two prominent disadvantages: device idle time (referred to as pipeline bubbles) and large activation memory. To eliminate pipeline bubbles, one line of work focuses on asynchronous PP [Gaunt et al., 2017, Harlap et al., 2018, Yang et al., 2021] which is theoretically bubble free. However, it sacrifices the exact optimization semantics and may result in lower convergence performance [Lian et al., 2018, Tang et al., 2020]. A

<sup>\*</sup>Equal Contributors.

<sup>†</sup>Work was done during an internship at Sea AI Lab.

parallel line of works revolve around synchronous PP, focusing on reducing pipeline bubbles and/or activation memory. GPipe [Huang et al., 2019] is a prominent early work to reduce the bubble rate by increasing the number of microbatches, at the cost of more activation memory. 1F1B [Fan et al., 2021] avoids the activation memory growth with respect to the number of microbatches by smartly staggering forward pass and backward pass, while keeping the same bubble rate with GPipe. Another notable work is GEMS [Jain et al., 2020], which stores activation memory of only one forward pass by scheduling microbatches one after another among two model replicas, thus with a significantly large bubble rate. Chimera [Li and Hoefer, 2021] extends the ideas of GEMS by combining two pipelines in different directions together, which reduces pipeline bubbles but with doubled parameter memory. In Megatron-LM [Narayanan et al., 2021], an interleaved strategy is proposed to further reduce the bubble rate, at the cost of more communication cost and a portion of extra activation memory. BPipe [Kim et al., 2023] focuses on reducing the activation memory of 1F1B from another perspective, transferring activation memory across devices based on the memory imbalance of 1F1B. However, it introduces a lot of extra communication and increases the complexity of the system, which makes it inefficient especially in settings with limited bandwidth. Zero Bubble [Qi et al., 2023] splits the backward into activation gradient computation and weight gradient computation, which can either reduce the pipeline bubbles without changing the maximum peak activation memory, or achieve zero bubble at the cost of doubled activation memory compared to 1F1B.

In this paper, we first demonstrate all existing pipelines can be seen as repeating a basic building block in time. We then identify a direct link between the activation memory and the lifespan of each building block, which reveals the core insight of this paper: lifespan decides the activation memory. Based on this insight, we present a family of novel and memory-efficient building blocks and their pipelines. Compared to 1F1B, we reduce the activation memory to 1/2 asymptotically with even higher throughput, and to 1/3 asymptotically with comparable throughput. We can also achieve zero bubble under the same activation memory with 1F1B. Notably, our strategy is almost a pure gain to the existing methods, only at the cost of doubled communication cost between pipeline stages, which is relatively small and can be neglected.

## 2 How to build a Pipeline

We propose a four-step framework to design pipeline schedules.

**Building Block:** It starts by laying out the passes for a single batch of data, which we call a *building block*. For example, the building block of the 1F1B schedule is made of a sequence of forward passes followed by backward passes in the reverse order. We highlight the building block of 1F1B in color in Figure 1a.

**Repeating:** More minibatches are then introduced. The building blocks are repeated and woven together to form a pipeline. In Figure 1 (top), the repeating building blocks are shown in different shades of grey. Notably, legit building blocks are required to repeat without a collision, namely, the passes from two building blocks should not overlap with each other.

**Squeezing:** Depending on the building block, there may be redundant bubbles in the pipeline, which can be simply removed by squeezing without changing the order of the passes. For example, figure 1b shows a case where squeezing produces a more efficient pipeline.

**Reordering (optional):** We can reorder the passes in the warm-up and cool-down phases to further improve the computation throughput. Intuitively, the peak of memory happens in the stable phase of the pipeline, while in the warm-up and cool-down phases the RAM is under utilized, leaving some space for improving the computation throughput without changing peak memory. We leave the details in Appendix C.

Most of the existing pipeline schedules can be explained under this framework. Besides the 1F1B and Eager 1F1B [Zhuang et al., 2023] shown in Figure 1, we show the interleaved 1F1B [Shoeybi et al., 2019], ZB-H1 [Qi et al., 2023] and a series of well-known pipeline in a more extensive gallery (see Appendix G).

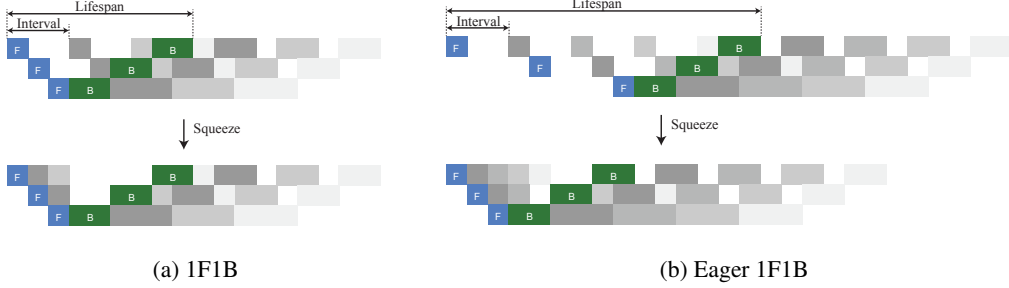


Figure 1: How to build a Pipeline

## 2.1 Building Blocks

The computation and memory efficiency of various pipelines can be attributed to their building blocks. The diversity of the building blocks primarily comes from three factors, **model partitioning**, **device placement**, and **offsets** between passes. We follow the idea and notations in zero bubble PP [Qi et al., 2023], using  $F$  to denote forward pass,  $B$  to denote “backward for the input”, and  $W$  to denote “backward for the weights”. Note that such finer granularity can be generalized to previous methods like 1F1B, by always grouping  $B$  and  $W$  together.

Model partitioning deals with how the model is divided into pipeline stages. The most common pattern is to equally divide the model to match the number of devices. A prominent example is the 1F1B schedule (Figure 1a). This is extended in interleaved 1F1B where the number of stages can be an integer multiple of the number of devices.

Device placement is another key factor in the design of building blocks. While conventionally each pipeline stage is sequentially placed on a different device, it is not uncommon to place multiple stages on the same device like in interleaved 1F1B. Another example of unconventional device placement is Chimera [Li and Hoefer, 2021], where two pipelines are placed in reversed device order.

Last but not least, the offsets between  $F, B, W$  passes play a major role in the computation and memory efficiencies of the pipeline. By simply enlarging the offsets between subsequent  $F$  passes in the building block of 1F1B, we obtain the eager 1F1B [Zhuang et al., 2023] (Figure 1b) where more  $F$  passes are eagerly scheduled, resulting in higher memory consumption. GPipe [Huang et al., 2019] can be seen as adding a large offset between the last  $F$  and the first  $B$  in the 1F1B building block. One more example on the effect of the offset is in the comparison of ZB-H1 and ZB-H2 schedules, one can see that properly chosen offsets result in zero bubble schedules like ZB-H2. In this work, we assume that every  $F$ ,  $B$  and  $W$  pass takes equally one unit of computation time, and only consider integer unit of offsets. Although this may limit the number of feasible building blocks, it greatly improves the simplicity of analysis.

## 2.2 Calculating the Peak Memory

Not every pipeline is born equal, researchers are constantly looking for pipelines that are more efficient in computation and/or memory. While efficient pipelines could be discovered by enumerating every possible building block, it is nonetheless prohibitively expensive. We discover that the peak memory consumption of a pipeline can be calculated from its building block via a simple formula. This enables us to design pipelines with a controllable peak memory.

Two quantities are crucial for the calculation of peak memory, the *lifespan* of a stage, and the repeating *interval* of the building blocks, both of which are illustrated in Figure 1. The lifespan of a stage is defined as the amount of time in between the starting of the  $F$  pass and the ending of  $B$  or  $W$  pass. A piece of activation memory is allocated at the starting of  $F$ , and retained in the RAM throughout the lifespan until it is consumed by both  $B$  and  $W$ . The peak memory consumption can be calculated by finding the maximum number of minibatches whose lifespans overlap with that of every other minibatch. Using  $l$  to denote lifespan,  $T$  to denote the repeating interval and  $m$  the size of activation memory for a single microbatch, we have the relation.

$$\text{peak memory} \leq \lceil \frac{l}{T} \rceil m$$

When there are multiple stages on one device, e.g. interleaved 1F1B, their contributions to the peak memory are independent, using  $S_i$  to denote all the stages allocated to device  $i$ , we sum the contributions from every stage.

$$\text{peak memory of device } i \leq \sum_{s \in S_i} \lceil \frac{l^s}{T} \rceil m^s \quad (1)$$

Another key insight is that the repeating interval  $T$  is readily determined from the building block. In an efficient pipeline,  $T$  should be equal to the number of units of computation in each stage of the building block. Any  $T$  larger than that would cause pipeline bubbles in the stable phase, and  $T$  smaller than that would lead to collisions. A subtle exception is the interleaved 1F1B whose repeating interval is not uniform. We leave the discussion to Appendix H.

### 2.3 Repeating without Collision

One constraint to keep in mind when designing the building blocks is that a legit building block is required to repeat without any collision. It may seem unintuitive how to design building blocks with this constraint. In practice, we design the building block first and perform a post-hoc verification. Another useful observation is that a legit building block usually produces a stable phase in the middle of pipeline, which contains a repeating  $d \times T$  rectangle, where  $d$  is the number of devices and  $T$  is the repeating interval. This offers an alternative to constrain the building blocks. We can start by ordering passes within this rectangle and convert it back to a building block.

## 3 Memory Efficient Building Blocks

With the above framework, we can conveniently analyse the memory consumption pattern of existing pipelines. To our knowledge, all existing pipelines are memory inefficient due to the imbalanced memory usage. The imbalanced memory comes from the innate heterogeneity of the lifespans across stages. From Figure 1a, we can easily see that the lifespan of the stages differs greatly from each other, with the first stage having the longest lifespan. Consequently, it causes a memory bottleneck on the first device and under utilization of memory on all other devices. To resolve this problem, we introduce a family of novel building blocks which we refer to as *V-Shape* building blocks. The insight of the V-Shape building block comes from Equation 1 which says that the peak memory depends on the sum of the lifespans. Therefore, when we place multiple stages on the same device, we should always collocate stages of long lifespans with those of short lifespans. When the total sum of lifespans is fixed, balanced placement always means higher memory efficiency. This can be demonstrated by Figure 2, the parallel schedule (used in interleaved 1F1B) is imbalanced and has a memory bottleneck proportional to  $l_1 + l_4$ , while in the V-Shape schedule it is  $l_1 + l_6$ .

The V-Shape schedule requests the model to be **partitioned** into stages twice the number of devices and the **device placement** of the second half of stages to be in reverse order as the first half. We can then further control the **offsets** between the passes to generate diverse building blocks. As the offsets directly determine the lifespan of each stage and therefore the peak memory by Equation 1, in the following, we introduce different V-Shape building blocks by their peak memory usage.

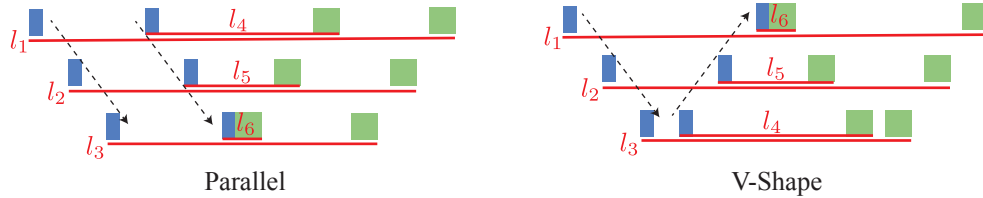


Figure 2: Parallel vs V-Shape.

### 3.1 V-Shape Building Blocks

Intuitively, in pipeline parallelism there is usually a trade-off between bubble rate and memory consumption [Qi et al., 2023], because we need more memory to fill in the warm-up and cool-down

bubbles. Following this intuition, we come up with 3 novel V-Shape building blocks with different memory consumption and bubble rate, controlled by different offsets in Figure 3. The building block of *V-Min* shown in Figure 3c has the minimum offsets thus the minimum memory consumption. Pushing to extreme throughput, *V-ZB* shown in Figure 3d can reduce bubble rate to 0. The building block of *V-Half* sits between the two extremes and consumes half of the activation memory needed by 1F1B. Note that although we show only 3 cases here, we can have a flexible memory consumption using the search algorithm illustrated in Appendix A.

We assume the model is uniformly partitioned, and use  $m$  to represent the activation memory of a single microbatch for each stage. We denote  $d$  as the number of devices,  $M$  as the total activation memory of the entire model for a single microbatch,  $l_{max} = \max_i (\sum_{s \in S_i} l^s)$  as the maximum total lifespan across all devices, we can analyse the lifespan and peak activation memory of 1F1B and V-Shape building blocks, shown in Table 1. Note that we ignored the constant terms when measuring  $l_{max}$  for simplicity in the analysis, e.g. accurately for *V-ZB*  $l_{max} = 12d - 2$  but we use  $l_{max} = 12d$  instead.

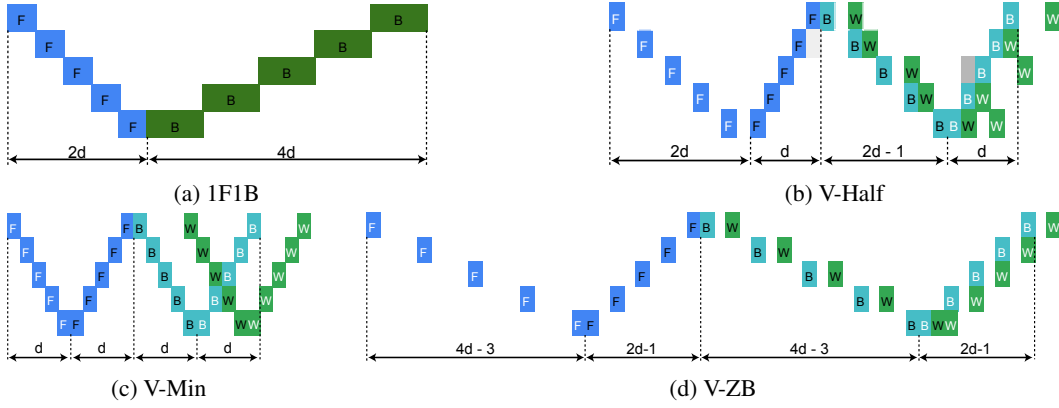


Figure 3: V-Shape Building Blocks.

Table 1: Activation Memory (Asymptotic) of V-Shape Building Blocks Compared to 1F1B

Building Block	Interval $T$	$l_{max}$	$m$	Peak Memory
1F1B	6	$6d$	$M/d$	$M$
<i>V-Min</i>	6	$4d$	$M/2d$	$M/3$
<i>V-Half</i>	6	$6d$	$M/2d$	$M/2$
<i>V-ZB</i>	6	$12d$	$M/2d$	$M$

Notably, to avoid collision the offsets in building block for *V-Min* and *V-Half* is slightly different on different  $d$ . The details are in Appendix F.

### 3.2 V-Shape Pipeline Schedules

Based on the framework in Section 2 and our V-Shape building blocks, we present the final schedules of *V-Min*, *V-Half* and *V-ZB* in Figure 4. Assuming  $F B W$  have equal run time, *V-Min* reduces the bubble rate to 2/3 of 1F1b, *V-Half* to 1/2 and while *V-ZB* achieves zero bubble similar to [Qi et al., 2023].

In real cases where  $F$ ,  $B$  and  $W$  may have different run times, *V-Min* suffers from a repeating bubble. As shown in Figure 5, there exists a bubble for every repeating interval  $T$ . As a result, the bubble grows with respect to the number of microbatches. Although *V-Half* may also encounter the same issue, we surprisingly find that it generates patterns that tessellates well in most empirical cases. As illustrated in Figure 5b, the throughput of *V-Half* is robust to the variation of run times. Additionally, we show that the bubbles of *V-ZB* will never grow when increasing the number of microbatches. We leave the related discussions in Appendix E.

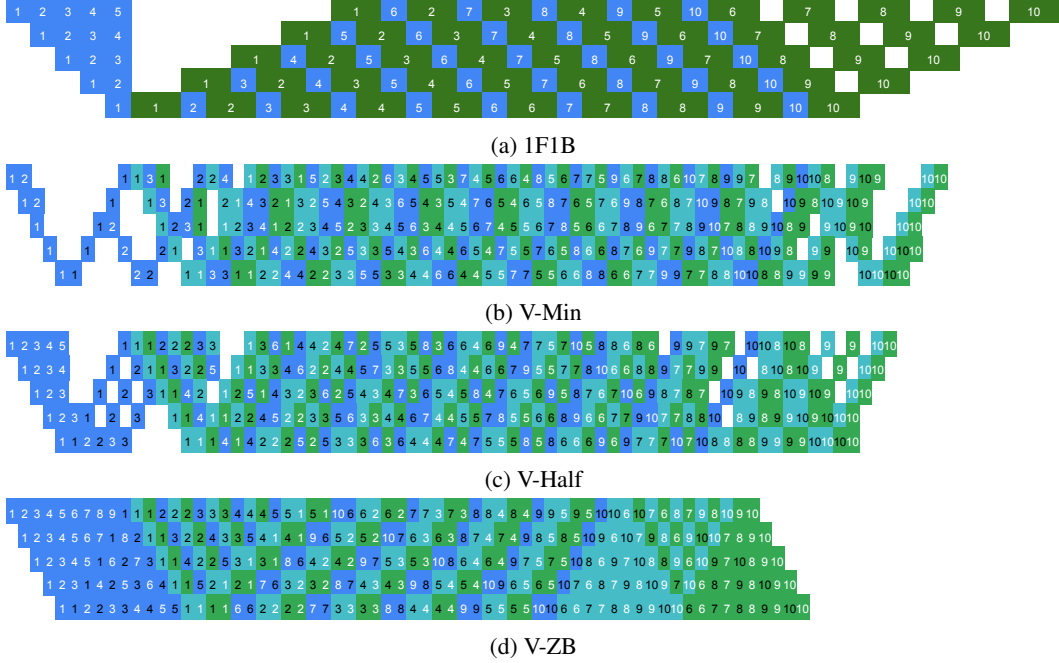


Figure 4: V-Shape Full Schedules.

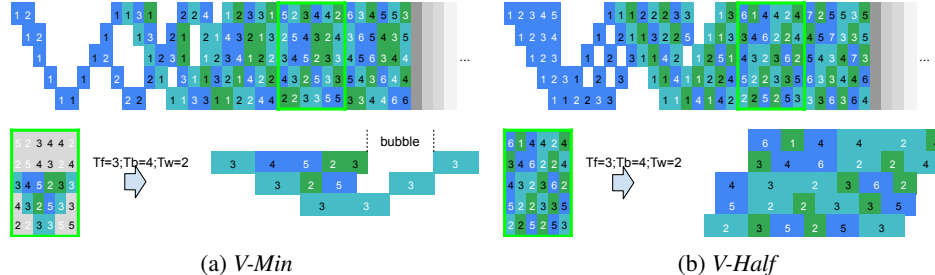


Figure 5: Repeating Bubble of *V-Min* compared to *V-Half*. We take a repeating  $d \times T$  grid from both schedule and assign  $F$   $B$   $W$  with different values. The result shows *V-Min* has a bubble for every repeating grid, while *V-Half* does not.

### 3.3 Other Building Blocks

Besides V-Shape building blocks, we also propose some other interesting building blocks (see Appendix I), to prove the generalization ability of our framework. Some useful examples include a) 1F1B-V achieving 2/3 of 1F1B’s activation memory without doing B-W split; b) a schedule with the same bubble rate as Interleaved 1F1B[Narayanan et al., 2021] but lower memory consumption.

## 4 Experiments

We construct our experiments to show three conclusions: a) The throughput and memory of *V-Min*, *V-Half* and *V-Min* aligns with the theoretical analysis in Section 3.2; b) Memory-saving methods including *V-Min* and *V-ZB* can bring acceleration; c) Our methods still perform best when combined with other state-of-the-art techniques.

### 4.1 Setup

We evaluate our methods using a series of models detailed in Table 2 analogous to GPT-3 [Brown et al., 2020]. Our implementation is based on open-source Megatron-LM project [Narayanan et al.,

2021] and is experimented on up to 40 NVIDIA A100 SXM 80G GPUs distributed across 4 nodes interconnected by a RoCE RDMA network. The running time of each iteration is recorded after several warm-up iterations. Similar to the settings in [Qi et al., 2023], we deduct one transformer layer from both the initial and final pipeline stages to compensate for the embedding or lm-head layers, which can otherwise become the bottleneck for the pipeline and interfere the efficiency.

Table 2: Models used in experiments

Model	Layers	Attention Heads	Hidden Size	GPUs
9.6B	30	40	5120	16
21B	46	48	6144	24
38.5B	62	64	7168	32
98.5B	78	80	10240	40

Our experiments majorly focuses on the following pipeline parallel schedules: 1) *V-Min*, *V-Half* and *V-ZB*: Schedules introduced in Section 3.2; 2) 1F1B and Interleaved 1F1B: Method implemented in Megatron-LM; 3) 1F1B-R: 1F1B used with full activation rematerialization; 4) ZB-1P and ZB-2P: The adaptive zero-bubble method introduced in [Qi et al., 2023] with activation memory limit set to the 1x/2x times of 1F1B.

## 4.2 Comparing Pipeline Schedules

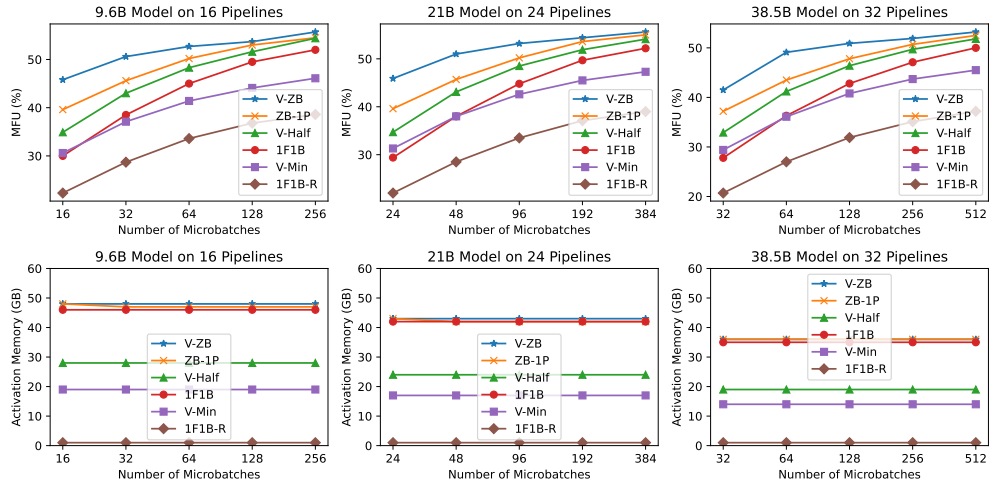


Figure 6: Throughput and activation memory using same micro batch size.

In Figure 6 we present a comparison of the throughput measured in FLOPS utilization (MFU) and activation memory consumption of each pipeline schedule using different settings, we find *V-ZB* outperforms all other methods, which aligns with Figure 4. When comparing the activation memory consumption, *V-Min* and *V-Half* stand out by significantly reducing activation memory to approximately 1/3 and 1/2, while other methods' memory is similar. More details of our experiments and definition of metrics can be found in Appendix D.1.

Notably we find *V-Min* has a comparable throughput against 1F1B, but its throughput falls behind 1F1B at a larger number of microbatch due to the aforementioned bubble in Figure 5a, as discussed in 3.2. However, it still outperforms 1F1B with full activation rematerialization, providing a strong alternative for saving memory.

We also plot both memory and MFU for the various methods in Figure 7 in a typical, but slightly different setting in which we reduced the microbatch size of 9.6B and 21B model to allow ZB-2P and Interleaved 1F1B to run which would otherwise run out of memory (OOM). It shows that the V-Shape pipeline schedules lie at the pareto frontier.

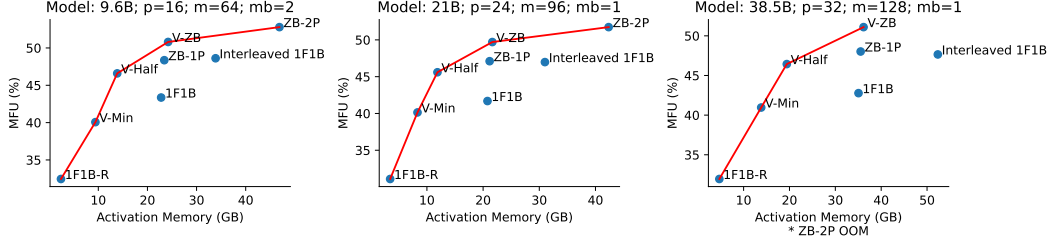


Figure 7: Pareto Frontier of MFU and Memory for Different Setup.

### 4.3 When to Save Memory

While *V-ZB* provides optimal throughput, *V-Half* and *V-Min* methods are mainly used when memory budget is tight. Conventionally, rematerialization is used when it runs out of memory (OOM). However, rematerialization leads to repeated computation and consequently decrease the throughput. *V-Half* and *V-Min* significantly outperforms rematerialization (1F1B-R) as we show in Table 7.

Another benefit of saving memory is that we can potentially use the extra memory for an increased microbatch size, which leads to a higher arithmetic intensity. We present the result in Figure 8. On bigger models, where memory pressure is higher and hence microbatch size is smaller, *V-Half* schedule can surpass *V-ZB* and other baselines because of its arithmetic intensity gain. This observation does not apply for *V-Min*, implying its arithmetic intensity gain can not compensate for the increased bubble. Doubling/Tripling the microbatch size for *V-Half*/*V-Min* results in a slightly higher activation memory than the other methods. This reflects the constant factors we ignored in Section 3.2. The increase is less significant as the number of devices grows.

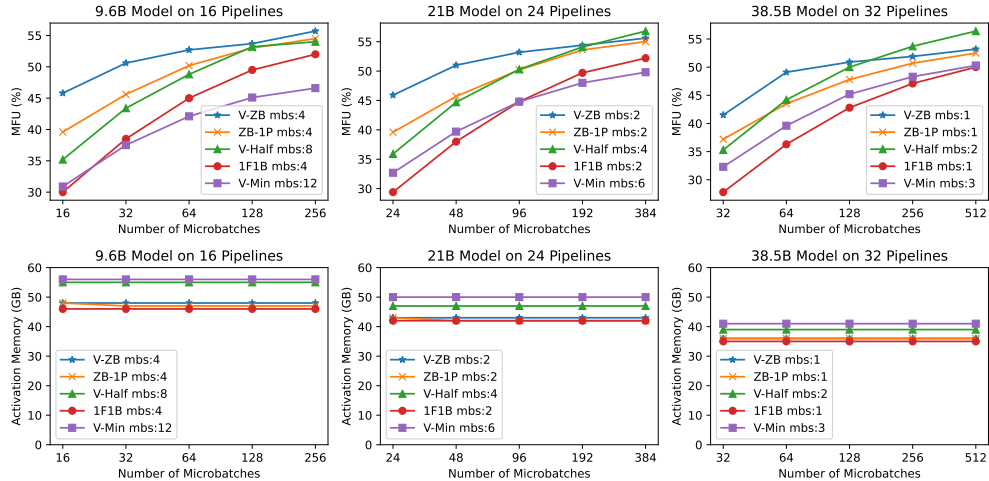


Figure 8: Throughput and activation memory under similar memory limit.

### 4.4 Combining with Existing Techniques

We present our method in the context of LLM training where it is used with various other techniques. The following techniques are considered: a) Flash Attention [Dao et al., 2022, Dao, 2023]; b) Tensor Parallel [Narayanan et al., 2021] and Sequence Parallel [Korthikanti et al., 2023]; c) Distributed Optimizer provided in Megatron-LM; The implementations are all from Megatron-LM [Narayanan et al., 2021]. Both our methods and the baseline methods are combined with the above techniques. Similar to the evaluation method in [Kim et al., 2023], we perform a grid search on the following parameters: the size of PP; the size of TP; the size of DP; the microbatch size ( $mb$ ). We use 40 GPUs in this experiment. For each method, the best result from the grid search is reported.

We present the best result for each pipeline parallel schedule in table 6 and the corresponding parameters. We find that when sequence length is smaller and hence the memory budget is more abundant, *V-ZB* performs the best due to the elimination of bubble. When we increase the sequence length and the number of microbatches, *V-Half* performs the best because of its memory efficiency. The detailed data and analysis of grid search can be found in the Appendix D.3.

Table 3: V Schedules Combined with Other Memory Saving Methods

Common Setup	PP Method	Best MFU (%)	Best Parameters			
			DP	TP	PP	mb
98.5B Model Seq Length 1024 Batch Size 160	1F1B	49.81	2	4	5	2
	1F1B-R	37.15	2	2	10	1
	ZB-1P	54.52	1	1	40	1
	V-Half	52.60	2	1	20	1
	V-Min	48.02	2	2	10	1
	V-ZB	57.58	1	1	40	1
98.5B Model Seq Length 3072 Batch Size 640	1F1B	57.25	2	4	5	1
	1F1B-R	45.81	2	1	20	1
	ZB-1P	56.55	1	4	10	1
	V-Half	60.34	1	2	20	1
	V-Min	55.51	1	1	40	1
	V-ZB	56.89	1	4	10	1

## 5 Conclusion And Future Work

In this work, we present a framework that designs pipeline parallel schedules by focusing on their repeating building blocks. We introduce a method to calculate peak activation memory from the building block. Based on this, we design a family of memory-efficient building blocks. We discuss and evaluate three representative methods from the family, namely *V-Min*, *V-Half* and *V-ZB*. We demonstrate with experiments that methods from this family advance the pareto frontier of throughput and memory in large model training, thereby accelerating the training of large models in practice. Furthermore, our methodology of designing pipeline schedules through building blocks may inspire the research community to explore more novel pipeline schedules in future works.

In the future, we plan to further explore more memory efficient pipeline schedules based on our framework. A prominent limitation of *V-Min* is that, it suffers from growing bubbles when increasing the number of microbatches. Although *V-Half* mitigates this issue, there is still a space to further reduce the memory consumption. Using continuous offsets or finer-granularity discretization is a promising way to solve it. We leave it in our future work.

## References

- Tom Brown, Benjamin Mann, Nick Ryder, Melanie Subbiah, Jared D Kaplan, Prafulla Dhariwal, Arvind Neelakantan, Pranav Shyam, Girish Sastry, Amanda Askell, et al. Language models are few-shot learners. *Advances in neural information processing systems*, 33:1877–1901, 2020.
- Tri Dao. Flashattention-2: Faster attention with better parallelism and work partitioning. *arXiv preprint arXiv:2307.08691*, 2023.
- Tri Dao, Dan Fu, Stefano Ermon, Atri Rudra, and Christopher Ré. Flashattention: Fast and memory-efficient exact attention with io-awareness. *Advances in Neural Information Processing Systems*, 35:16344–16359, 2022.
- Shiqing Fan, Yi Rong, Chen Meng, Zongyan Cao, Siyu Wang, Zhen Zheng, Chuan Wu, Guoping Long, Jun Yang, Lixue Xia, et al. Dapple: A pipelined data parallel approach for training large models. In *Proceedings of the 26th ACM SIGPLAN Symposium on Principles and Practice of Parallel Programming*, pages 431–445, 2021.

- Alexander L Gaunt, Matthew A Johnson, Maik Riechert, Daniel Tarlow, Ryota Tomioka, Dimitrios Vytiniotis, and Sam Webster. Ampnet: Asynchronous model-parallel training for dynamic neural networks. *arXiv preprint arXiv:1705.09786*, 2017.
- Priya Goyal, Piotr Dollár, Ross Girshick, Pieter Noordhuis, Lukasz Wesolowski, Aapo Kyrola, Andrew Tulloch, Yangqing Jia, and Kaiming He. Accurate, large minibatch sgd: Training imagenet in 1 hour. *arXiv preprint arXiv:1706.02677*, 2017.
- Aaron Harlap, Deepak Narayanan, Amar Phanishayee, Vivek Seshadri, Nikhil Devanur, Greg Ganger, and Phil Gibbons. Pipedream: Fast and efficient pipeline parallel dnn training. *arXiv preprint arXiv:1806.03377*, 2018.
- Yanping Huang, Youlong Cheng, Ankur Bapna, Orhan Firat, Dehao Chen, Mia Chen, HyoukJoong Lee, Jiquan Ngiam, Quoc V Le, Yonghui Wu, et al. Gpipe: Efficient training of giant neural networks using pipeline parallelism. *Advances in neural information processing systems*, 32, 2019.
- Arpan Jain, Ammar Ahmad Awan, Asmaa M Aljuhani, Jahanzeb Maqbool Hashmi, Quentin G Anthony, Hari Subramoni, Dhableswar K Panda, Raghu Machiraju, and Anil Parwani. Gems: Gpu-enabled memory-aware model-parallelism system for distributed dnn training. In *SC20: International Conference for High Performance Computing, Networking, Storage and Analysis*, pages 1–15. IEEE, 2020.
- Taebum Kim, Hyoungjoo Kim, Gyeong-In Yu, and Byung-Gon Chun. Bpipe: Memory-balanced pipeline parallelism for training large language models. In *International Conference on Machine Learning*, pages 16639–16653. PMLR, 2023.
- Vijay Anand Korthikanti, Jared Casper, Sangkug Lym, Lawrence McAfee, Michael Andersch, Mohammad Shoeybi, and Bryan Catanzaro. Reducing activation recomputation in large transformer models. *Proceedings of Machine Learning and Systems*, 5, 2023.
- Shigang Li and Torsten Hoefer. Chimera: efficiently training large-scale neural networks with bidirectional pipelines. In *Proceedings of the International Conference for High Performance Computing, Networking, Storage and Analysis*, pages 1–14, 2021.
- Xiangru Lian, Wei Zhang, Ce Zhang, and Ji Liu. Asynchronous decentralized parallel stochastic gradient descent. In *International Conference on Machine Learning*, pages 3043–3052. PMLR, 2018.
- Deepak Narayanan, Mohammad Shoeybi, Jared Casper, Patrick LeGresley, Mostofa Patwary, Vijay Korthikanti, Dmitri Vainbrand, Prethvi Kashinkunti, Julie Bernauer, Bryan Catanzaro, et al. Efficient large-scale language model training on gpu clusters using megatron-lm. In *Proceedings of the International Conference for High Performance Computing, Networking, Storage and Analysis*, pages 1–15, 2021.
- Penghui Qi, Xinyi Wan, Guangxing Huang, and Min Lin. Zero bubble pipeline parallelism. In *The Twelfth International Conference on Learning Representations*, 2023.
- Mohammad Shoeybi, Mostofa Patwary, Raul Puri, Patrick LeGresley, Jared Casper, and Bryan Catanzaro. Megatron-lm: Training multi-billion parameter language models using model parallelism. *arXiv preprint arXiv:1909.08053*, 2019.
- Zhenheng Tang, Shaohuai Shi, Wei Wang, Bo Li, and Xiaowen Chu. Communication-efficient distributed deep learning: A comprehensive survey. *arXiv preprint arXiv:2003.06307*, 2020.
- Bowen Yang, Jian Zhang, Jonathan Li, Christopher Ré, Christopher Aberger, and Christopher De Sa. Pipemare: Asynchronous pipeline parallel dnn training. *Proceedings of Machine Learning and Systems*, 3:269–296, 2021.
- Lianmin Zheng, Zhuohan Li, Hao Zhang, Yonghao Zhuang, Zhifeng Chen, Yanping Huang, Yida Wang, Yuanzhong Xu, Danyang Zhuo, Eric P Xing, et al. Alpa: Automating inter-and {Intra-Operator} parallelism for distributed deep learning. In *16th USENIX Symposium on Operating Systems Design and Implementation (OSDI 22)*, pages 559–578, 2022.
- Yonghao Zhuang, Lianmin Zheng, Zhuohan Li, Eric Xing, Qirong Ho, Joseph Gonzalez, Ion Stoica, Hao Zhang, and Hexu Zhao. On optimizing the communication of model parallelism. *Proceedings of Machine Learning and Systems*, 5, 2023.

## A Adaptive Scheduler Based on Search

Now we consider more general scenarios, where we want to minimize the bubbles given an activation memory limit  $M_{\text{limit}}$ . A straightforward approach should be simply searching over all possible offsets and picking the one with minimal bubbles. However, this naive method cannot work well due to there are exponentially many possible offsets, which makes it intractable to iterate thoroughly. In this section, we propose a more practical searching method to solve this general problem.

We use superscript  $c \in \{0, 1\}$  to denote which chunk in a device, and use subscript  $i \in \{1, 2, \dots, d\}$  to denote the index of the device. For example,  $F_i^c$  represent the forward pass of chunk  $c$  in the  $i$ -th device. We define the offset from  $u$  to  $v$  as  $\delta(u, v) = t(v) - t(u)$ , where  $t(v)$  represent the cell index along time horizon of pass  $v$ . To simplify the notations, we define  $\delta F_i^0 = \delta(F_i^0, F_{i+1}^0)$ ,  $\delta F_i^1 = \delta(F_i^1, F_{i-1}^1)$ ,  $\delta B_i^1 = \delta(B_i^1, B_{i+1}^1)$  and  $\delta B_i^0 = \delta(B_i^0, B_{i-1}^0)$ , to denote the offset from a pass to its next pass.

Instead of all possible offsets, we limit our search space to uniform offset across devices. We also try to ensure each device has a balanced lifespan and peak memory. To make it work for a finer granularity of memory controlling, we split the repeating module into two parts, containing the first  $K$  rows and the last  $d - K$  rows respectively. More formally, we use the constraint as follows.

$$\begin{aligned} \delta F_i^0 = \delta B_i^1 &= \delta_{<K}^0, \forall 1 \leq i < K & \delta F_i^1 = \delta B_i^0 &= \delta_{\leq K}^1, \forall 1 < i \leq K \\ \delta F_i^0 = \delta B_i^1 &= \delta_{\geq K}^0, \forall K \leq i < d & \delta F_i^1 = \delta B_i^0 &= \delta_{>K}^1, \forall K < i \leq d \end{aligned} \quad (2)$$

Note that the above constraints have good properties that 1) lifespan is balanced across chunks and pipeline stages; 2) peak memory is balanced across pipeline stages. As we can always greedily fill  $W_i^0$  and  $W_i^1$  when repeating, we only need to search over the permutation of the first device, the values of  $\delta_{<K}^0, \delta_{\leq K}^1, \delta_{\geq K}^0, \delta_{>K}^1$  and  $K$ . The computational complexity is  $O(d)$  if we regard repeating interval as a constant.

For each building block searched, we repeat the building block, check collision, do squeezing and reordering as mentioned in 2.1. After searching over all possible building blocks, we pick the schedule with minimal bubbles. Note that we can use the true run times of  $F$ ,  $B$  and  $W$  to calculate the bubbles, which will lead to more efficient schedule in real cases.

## B Bubble Rate Evaluation of Adaptive Scheduler

In Figure 9 we show the bubble rate of adaptive V-Shape schedulers introduced in A under different settings and different memory limit. The run times of  $F$ ,  $B$  and  $W$  are from profiled real cases, as in Table 5. We observe that the bubble rate drops as memory limit increases. Notably, there's a sudden drop of bubble rate when the memory limit just goes above approximately 1/2 of 1F1B, at which point the per-microbatch bubble mentioned in Figure 5a disappears.

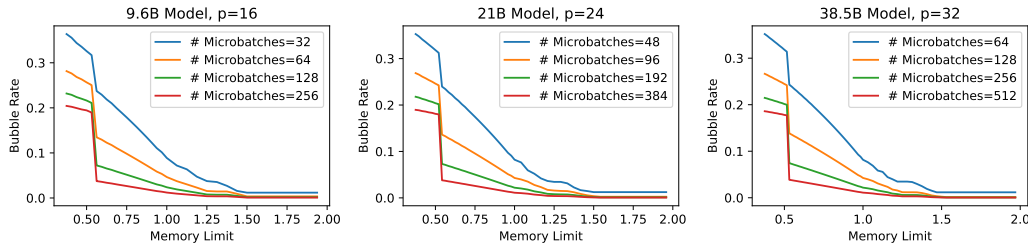


Figure 9: Bubble Rate of V Scheduler under Different Settings.

We also compare V scheduler with the adaptive zero bubble scheduler proposed in [Qi et al., 2023] in Figure 10. We find that V scheduler has a boarder range of memory configurations and a smaller bubble rate compared to zero bubble scheduler. We also draw the bubble rate of 1F1B as a reference, though 1F1B does not support a configurable memory.

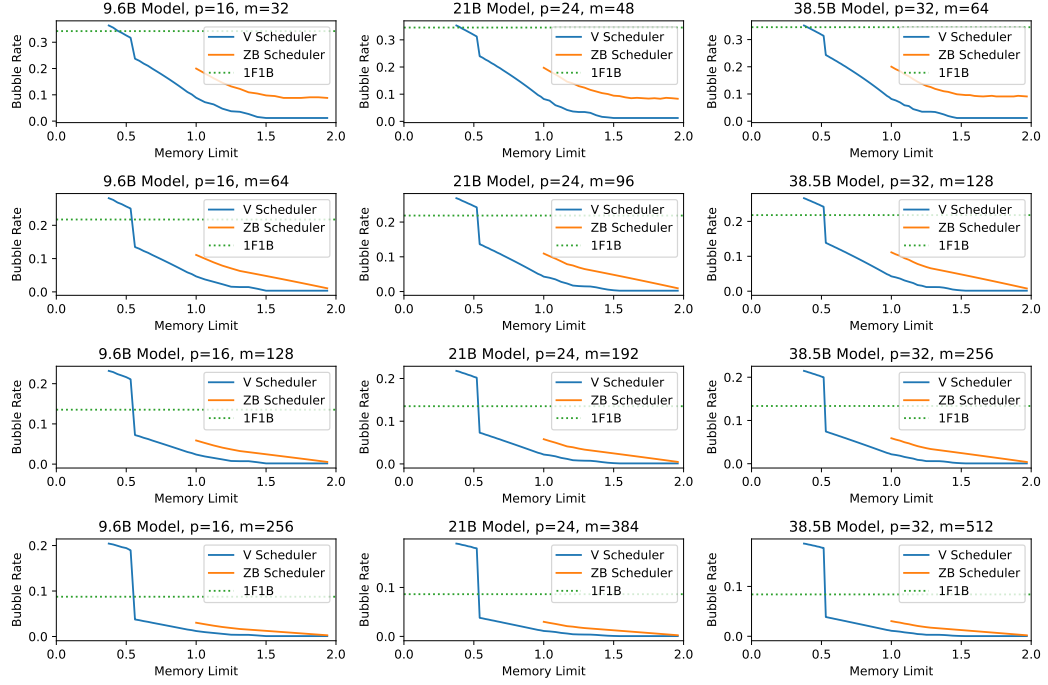


Figure 10: Comparison of V Scheduler and Zero Bubble Scheduler.

## C Reordering

In our framework, we may need to reorder the warm-up and cool-down phases after squeezing. We employ simple greedy approaches to handle the reordering for warm-up and cool-down, and illustrate how zero bubble schedule is reordered in Figure 11.

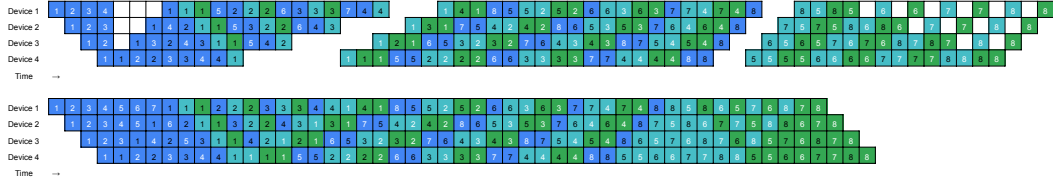


Figure 11: Top: the schedule after **Squeezing**. Bottom: the schedule after **Reordering**.

**Warm-up** In warm-up phase, bubbles mainly happen before the first  $B$ . We iterate all the cells from left to right. If a vacant cell (which means a bubble) is encountered, we try to find a computation pass to fill this bubble. We iterate all the following computation passes in the same stage, and check whether it is possible to move if we keep all other passes unchanged. If the check succeeds, we move it to the vacant cell, and the bubble is filled.

**Cool-down** In cool-down phase,  $W$  can be scheduled at any time after its corresponding  $B$ . So we utilize a heuristic way to handle the bubbles. Firstly, we delete all the  $W$  passes in cool-down phase. Next, we squeeze the schedule to remove the bubbles caused by deleting  $W$ . After that, we use  $W$  to fill the remaining bubbles, ensuring each  $W$  is after its corresponding  $B$ . Finally, we schedule all the remaining  $W$  passes at the end.

## D Detailed Experiment Data

### D.1 Comparing Pipeline Schedules

For Section 4.2, we present our detailed experiment data in Table 4. Specifically the metrics are defined as:

- MFU: The FLOPS utilization of the training system. The calculation of FLOPS of a model is following [Narayanan et al., 2021].
- Total Memory: The maximum peak memory cross all devices.
- Activation Memory: Estimated as deducting the iteration-start memory from peak memory on each device. The number presented is the maximum activation memory cross all devices.
- Bubble Rate: The theoretical bubble rate reported by scheduler, using profiled run times of  $F$ ,  $B$  and  $W$  at starting iterations.

Table 4: Comparing Pipeline Schedules

Setup	Model	9.6B					21B					38.5B				
		16					24					32				
	Microbatch	4					2					1				
		#GPU	16	32	64	128	256	24	48	96	192	384	32	64	128	256
Samples per second per GPU	V-ZB	2.59	2.86	2.98	3.04	3.15	1.19	1.32	1.38	1.41	1.44	0.59	0.70	0.72	0.74	0.76
	ZB-1P	2.24	2.58	2.84	2.99	3.08	1.02	1.18	1.30	1.39	1.43	0.53	0.62	0.68	0.72	0.75
	V-Half	1.97	2.43	2.73	2.92	3.08	0.90	1.12	1.26	1.34	1.40	0.47	0.58	0.66	0.71	0.74
	1F1B	1.69	2.18	2.55	2.80	2.94	0.76	0.99	1.16	1.29	1.35	0.40	0.52	0.61	0.67	0.71
	V-Min	1.73	2.10	2.34	2.49	2.61	0.81	0.98	1.10	1.18	1.22	0.42	0.51	0.58	0.62	0.65
	1F1B-R	1.26	1.62	1.90	2.08	2.18	0.57	0.74	0.87	0.96	1.01	0.29	0.38	0.45	0.50	0.53
MFU (%)	V-ZB	45.8	50.6	52.7	53.7	55.7	45.9	51.0	53.2	54.4	55.6	41.5	49.1	50.9	51.9	53.2
	ZB-1P	39.6	45.6	50.2	53.0	54.5	39.6	45.7	50.2	53.6	55.0	37.2	43.5	47.8	50.7	52.5
	V-Half	34.9	43.0	48.3	51.6	54.4	34.7	43.1	48.5	51.9	54.1	32.9	41.2	46.4	49.7	51.8
	1F1B	30.0	38.5	45.0	49.5	52.0	29.4	38.0	44.8	49.7	52.2	27.8	36.3	42.8	47.1	50.0
	V-Min	30.6	37.1	41.4	44.1	46.1	31.3	38.0	42.6	45.5	47.3	29.4	36.1	40.8	43.7	45.5
	1F1B-R	22.3	28.7	33.6	36.8	38.6	22.0	28.5	33.5	37.1	39.0	20.7	27.0	31.9	35.1	37.2
Total memory (GB)	V-ZB	58	59	59	59	59	57	57	57	57	57	55	55	55	55	55
	ZB-1P	58	57	57	57	57	57	56	56	56	56	55	55	55	55	55
	V-Half	38	38	38	38	38	38	38	38	38	38	38	38	38	38	38
	1F1B	56	56	56	56	56	56	56	56	56	56	54	54	54	54	54
	V-Min	29	29	29	29	29	31	31	31	31	31	33	33	33	33	33
	1F1B-R	14	14	14	14	14	18	18	18	18	18	24	24	24	24	24
Activation memory (GB)	V-ZB	48	48	48	48	48	43	43	43	43	43	36	36	36	36	36
	ZB-1P	48	47	47	47	47	43	42	42	42	42	36	36	36	36	36
	V-Half	28	28	28	28	28	24	24	24	24	24	19	19	19	19	19
	1F1B	46	46	46	46	46	42	42	42	42	42	35	35	35	35	35
	V-Min	19	19	19	19	19	17	17	17	17	17	14	14	14	14	14
	1F1B-R	1	1	1	1	1	1	1	1	1	1	1	1	1	1	1
Bubble rate (%)	V-ZB	18.7	8.88	4.57	2.32	1.16	18.9	8.51	4.39	2.19	1.09	18.7	8.61	4.3	2.24	1.14
	ZB-1P	31.7	20.1	11.2	5.92	3.06	31.5	19.8	11.0	5.82	3.0	32.1	20.1	11.1	5.89	3.04
	V-Half	40.5	24.2	13.8	7.41	3.84	41.3	24.6	14.0	7.5	3.89	42.0	24.9	14.3	7.6	3.97
	1F1B	50.1	34.3	21.7	13.5	8.76	50.5	34.6	21.9	13.5	8.67	50.7	34.6	21.8	13.4	8.44
	V-Min	48.4	36.5	28.0	23.1	20.3	47.8	35.8	27.4	21.9	19.1	48.6	36.5	27.8	22.5	19.5
	1F1B-R	50.1	34.3	21.7	13.5	8.76	50.5	34.6	21.9	13.5	8.67	50.7	34.6	21.8	13.4	8.44

## D.2 Single-pass MFU Gain When Increasing Microbatch Size

To evaluate how increasing microbatch size increases arithmetic intensity, we profile the run time of each single F/B/W pass and calculate their single-pass MFU. We list the result in Table 5. It shows that whether there’re significant MFU gain depends on both the model and current microbatch size.

Table 5: Single-pass MFU Gain When Increasing Microbatch Size

Model	9.6B			21B			38.5B		
	4	8	12	2	4	6	1	2	3
F Pass (ms)	12.96	26.30	39.45	9.30	18.11	26.81	6.72	12.27	18.05
B Pass (ms)	13.22	26.66	39.85	9.47	18.55	27.09	6.89	12.84	18.73
W Pass (ms)	9.76	19.62	28.93	7.19	14.03	21.82	5.06	9.63	15.46
FBW Average MFU (%)	65.6	64.98	65.36	64.68	66.24	66.52	60.81	65.37	65.2

## D.3 More Details on Grid Search

We show the MFU of every setup of our grid search in Table 6 and 7 for two groups experiments: one with  $SequenceLength = 1024$  and  $BatchSize = 160$ , another with  $SequenceLength = 3072$  and  $BatchSize = 640$ .

For the first experiment group, the best setup is *V-ZB* under pure PP because of its bubble elimination. For the second setup, the best setup is *V-Half* because its memory efficiency enables a lower TP degree which is otherwise impossible for *V-ZB/ZB-1P/1F1B*. A comparison of TP and PP can be found at D.4.

Table 6: Raw MFU Data of Grid Search

Parallelisation	MicroBS	1F1B	1F1B-R	ZB-1P	V-Half	V-Min	V-ZB
DP=1	1	46.99	34.72	47.83	47.59	43.07	48.58
TP=4	2	49.11	36.67	51.27	50.86	45.69	52.98
PP=10	4	47.69	35.3	-	50.46	45.29	-
DP=2	1	49.26	37.15	52.08	51.7	48.02	53.69
TP=2	2	-	36.7	-	51.87	47.56	-
PP=10	4	-	31.96	-	-	-	-
DP=1	1	49.14	36.88	52.43	51.73	46.02	54.19
TP=2	2	48.47	36.22	52.34	51.75	45.84	54.78
PP=20	4	-	31.48	-	-	41.4	-
DP=2	1	-	36.69	-	52.6	48.0	-
TP=1	2	-	32.64	-	-	44.41	-
PP=20	4	-	25.27	-	-	-	-
DP=1	1	48.63	36.44	54.52	52.46	47.78	57.58
TP=1	2	-	32.46	-	49.19	43.91	-
PP=40	4	-	25.04	-	-	-	-
DP=1	1	40.66	30.2	40.56	40.07	33.54	41.22
TP=8	2	47.07	35.17	47.9	47.24	41.26	48.45
PP=5	4	47.3	35.01	48.96	48.19	42.45	49.09
	8	45.66	33.5	-	47.17	42.59	-
DP=2	1	46.89	35.22	48.55	47.79	44.3	48.75
TP=4	2	49.81	37.01	52.27	51.22	47.51	52.79
PP=5	4	-	36.03	-	51.41	47.43	-

## D.4 Model Parallelism: More PP or More TP?

Our grid search result in Appedix D.3 shows a strong favor of Pipeline Parallel (PP) over Tensor Parallel (TP), which might contradict with some existing industry experience from which some degree

Table 7: Raw MFU Data of Grid Search on Increased Sequence Length and Batch Size

Parallelisation	MicroBS	1F1B	1F1B-R	ZB-1P	V-Half	V-Min	V-ZB
d=1	1	56.45	41.7	56.55	56.54	51.19	56.89
t=4	2	-	41.4	-	41.71	50.52	-
p=10	4	-	41.24	-	-	-	-
d=2	1	-	44.59	-	-	55.11	-
t=2	2	-	43.1	-	-	-	-
p=10	4	-	41.25	-	-	-	-
d=1	1	-	44.23	-	60.34	52.68	-
t=2	2	-	42.91	-	-	-	-
p=20	4	-	41.2	-	-	-	-
d=2	1	-	45.81	-	-	-	-
t=1	2	-	41.85	-	-	-	-
p=20	4	-	-	-	-	-	-
d=1	1	-	45.2	-	-	55.51	-
t=1	2	-	41.16	-	-	-	-
p=40	4	-	38.86	-	-	-	-
d=1	1	50.87	37.57	49.23	49.31	45.25	49.46
t=8	2	52.42	38.54	50.25	50.6	47.18	50.71
p=5	4	-	39.38	-	-	13.27	-
d=2	1	57.25	42.28	-	56.35	52.51	-
t=4	2	-	41.76	-	-	-	-
p=5	4	-	40.42	-	-	-	-

of TP usually accelerates training. To understand the reason we briefly compare TP and PP in this section.

Though PP also equally shards activation memory to  $p$  PP shards, it usually needs to cache  $\Theta(p)$  activation memory, resulting in a total activation memory demand same as the unsharded. On the other hand, TP, when used with sequence parallel, shards most activation memory equally to  $t$  TP shards, which is one of the most significant benefit of TP over PP. However, this comes at the cost of reducing the dimensions of hidden size to  $\frac{1}{t}$ , which can significantly decrease the single-pass (F/B/W) MFU. Though one can argue that the saved memory can be used to increase the minibatch size, our experiment also measured the MFU under different TP setups in Table 12 demonstrates that a higher-degree of TP even with higher minibatch size still suffers from lower single-pass MFU.

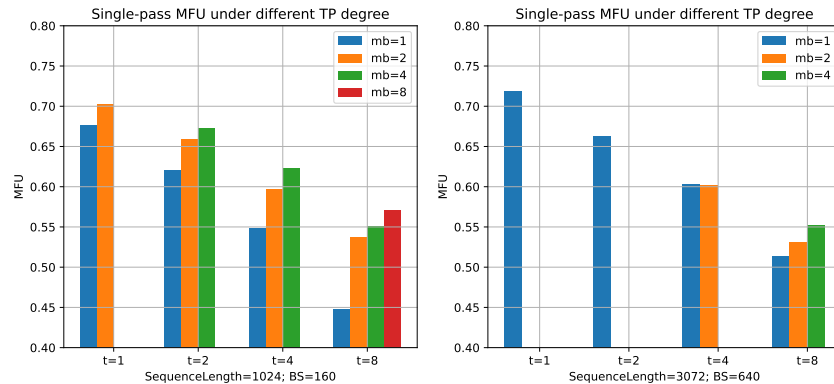


Figure 12: Average Single-pass MFU (FBW Average) for Grid Search Under Different TP Degrees

The throughput of PP also decreases as PP degree increases for two major reasons: 1) For baseline PP schedules with pipeline bubbles and a fixed global batch size, having a higher PP degree usually results in higher pipeline bubbles. For example 1F1B has a bubble rate of  $\frac{p-1}{p+n-1}$  which significantly increases if  $p$  grows and  $n$  keeps unchanged. 2) The first and the last pipeline stage for a transformer

model usually have an embedding or lm-head which has nonnegligible additional computations, making the pipeline unbalanced. If we have a transformer model with  $l$  layers spread on  $p$  pipeline stages, while the FLOPS of lm-head or embedding is equal to  $k$  transformer layers, then a roughly  $\frac{k}{\frac{l}{p} + k}$  bubble rate is introduced, which increases with  $p$ . However these two problems can be mitigated. For problem 1 a setting with a bigger number of microbatches or using *V-ZB* can significantly reduce the pipeline bubble. For problem 2 we can use another standalone stage to handle the embedding or lm-head instead if we need to keep the number of transformer layers of the entire model unchanged. In our experiments for simplicity we deducted 1 layer from both the first and last pipeline stage to mitigate this problem.

As a result, our methods and setup essentially pushes our preference from TP to PP, majorly because a lower degree of TP has higher single-pass MFU

## E Bubble Analysis

Although we mainly focus on the memory efficiency in this paper, we also need to take care of the bubbles in pipeline parallelism. Typically, there is a trade-off between memory and bubble (refer to [Qi et al. \[2023\]](#)), where allowing more memory usage can reduce the bubble of a pipeline schedule. In this section, we will discuss how to identify whether the bubble of a schedule will grow with respect to the number of microbatches. Additionally, we illustrate an empirical lower bound of bubble in our methods.

### E.1 $O(p)$ or $O(n)$

In pipeline parallelism, we usually expect the bubble is only related to the number of pipeline devices ( $p$ ), and won't grow when increasing the number of microbatches ( $n$ ). This property guarantees a good scalability with respect to  $n$ . We say a pipeline schedule is with  $O(p)$  bubble if it satisfies this property, otherwise with  $O(n)$  bubble. Note that the conclusion is based on the values of  $T_F$ ,  $T_B$  and  $T_W$ , which are the run times of  $F$ ,  $B$  and  $W$  respectively. For example, the schedule in Figure 4b is with  $O(p)$  bubble when  $T_F = T_B = T_W$ , but is with  $O(n)$  bubble when  $T_W$  is significantly smaller than  $T_F$  and  $T_B$ .

**If a schedule is with  $O(p)$  bubble for any values of  $T_F, T_B, T_W$ , the minimal memory is  $2p\bar{m}$ .** In a pipeline schedule, there are two types of dependencies, streaming dependency within the same stage and computational dependency across stages. We define a dependency path as a sequence of passes  $\tau = (v_1, v_2, \dots, v_{|\tau|})$  where for any  $1 < i \leq |\tau|$ ,  $v_i$  is dependent on  $v_{i-1}$  (either streaming dependency or computational dependency). We define the time cost of a dependency path as  $T_\tau = \sum_{1 \leq i \leq |\tau|} T_{v_i}$  where  $T_{v_i}$  is the time cost of  $v_i$ . Then the runtime of the whole pipeline should be  $T = \max_\tau T_\tau$ .

Obviously, there is a trivial dependency path  $\tau_1$  that all the passes are from the same stage, and  $T_{\tau_1} = 2n(T_F + T_B + T_W)$ . Note that it is the lower bound of runtime, and any extra runtime would be considered as bubbles.

Let's consider another dependency path  $\tau_2$  containing only forward passes. To be simple, we denote  $\hat{F}_j$  as the forward sequence for the  $j$ -th microbatch. Then  $\tau_2 = \text{concatenate}(\hat{F}_0, \hat{F}_k, \dots, \hat{F}_{\lfloor \frac{n-1}{k} \rfloor k})$  and  $T_{\tau_2} = 2p \lfloor \frac{n+k-1}{k} \rfloor T_F$ , where  $6k > \delta(F_1^0, F_1^1) > 6(k-1)$  (greedily include as many forward passes as possible). Note that if we want to make  $O(p)$  bubbles for any values of  $T_F, T_B, T_W$ , we should choose  $k \geq p$  to make  $2p \lfloor \frac{n+k-1}{k} \rfloor \leq 2n$ , otherwise  $2p \lfloor \frac{n+k-1}{k} \rfloor T_F - 2n(T_F + T_B + T_W) \in O(n)$  if we set  $T_B = T_W = 0$ . Then we can get  $\delta(F_1^0, F_1^1) > 6p - 6$ .

Then we consider a similar dependency path  $\tau_3$  containing only backward passes and we can get  $\delta(B_1^1, B_1^0) > 6p - 6$ . According to Formula 1, we can get the peak memory in the first stage is at least  $(\lceil \frac{\delta(F_1^0, F_1^1)}{6} \rceil + \lceil \frac{\delta(B_1^1, B_1^0)}{6} \rceil) \bar{m} \geq 2p\bar{m}$ .

**For most real cases,  $p\bar{m}$  is enough to guarantee  $O(p)$  bubble.** Although the above proof shows that  $2p\bar{m}$  memory is required to guarantee  $O(p)$  bubble for any values of  $T_F, T_B, T_W$ , we don't need that much memory in practice because the values of  $T_F, T_B$  and  $T_W$  are well constrained. As in [Qi](#)

et al. [2023],  $F$ ,  $B$  and  $W$  have similar total FLOPS, and  $T_F, T_B, T_W$  don't differ too much in real cases. Based on this insight, we can check the conditions where our methods are with  $O(p)$  bubble.

Because both warm-up phase and cool-down phase have  $O(p)$  passes, we only need to consider the stable phase to identify whether a schedule is with  $O(p)$  bubble or with  $O(n)$  bubble. Obviously, streaming dependency won't block the device from executing next pass. So bubble is caused only by the computational dependency. Formally, a schedule is with  $O(n)$  bubble if and only if there exist two passes  $u$  and  $v$  (within the same stage) and there are two dependency paths  $\tau$  and  $\tau'$  between them, where  $\tau$  only contains streaming dependencies,  $\tau'$  contains at least two computational dependencies, and  $T_\tau < T_{\tau'}$ . Based on our V-shape building blocks, we only need to check  $u$  and  $v$  with a small distance ( $< 6$ ) and  $\tau'$  within two adjacent stages. In this way, we can conclude that the schedule in Figure 4c is with  $O(p)$  bubble when  $T_W + 2T_B \geq 2T_F$  &  $T_W + 2T_F \geq 2T_B$ , which is satisfied in most real cases.

## E.2 Lower Bound

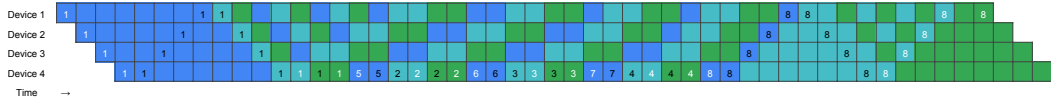


Figure 13: A dependency path of pipeline schedule.

The runtime of a schedule can be bounded by any dependency path. In Figure 13, we present a dependency path which is a non-trivial lower bound for most schedules after squeezing and reordering. Assuming the actual peak memory is  $k\bar{m}$  ( $k \leq 2p$ ) and  $T_F = T_B = T_W = 1$ , then the runtime of this dependency path is at least  $6n + 6p - 3k - 1$ . Empirically, we find that we can always get close to this lower bound in our adaptive scheduler.

## F Building Blocks of *V-Min* and *V-Half* for all values of $d$

To avoid collisions between the repeating building blocks, we'll need a slightly different offsets for different number of devices  $d$ . We list the details in Table 8 and 9 while continue using the notation defined in A. We didn't list the offsets related to  $W$  passes because they always fill in the empty grids left by  $F$  and  $B$ . Some samples can also be found at Figure 14.

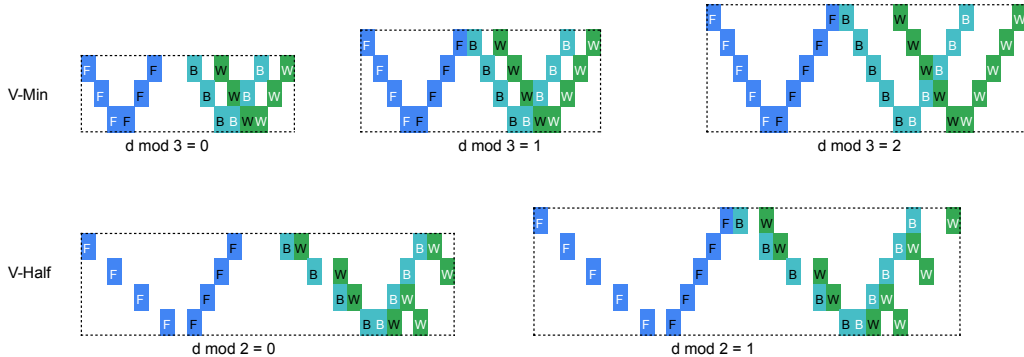


Figure 14: Building Blocks of *V-Min* and *V-Half* on Different Settings of  $d$

Table 8: Offsets for *V-Min*

$0 \leq i < d, 0 < j \leq d$	$\delta F_i^0$	$\delta F_j^1$	$\delta B_i^0$	$\delta B_j^1$	$\delta(F_d^0, F_d^1)$	$\delta(F_0^1, B_0^1)$	$\delta(B_d^0, B_d^1)$
$0 \equiv d \pmod{3}$	1	1	1	1	1	3	1
$0 < d \pmod{3}$	1	1	1	1	1	1	1

Table 9: Offsets for *V-Half*

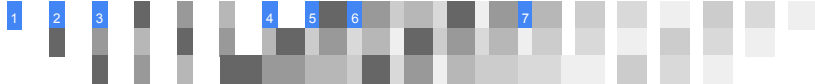
$0 \leq i < d, 0 < j \leq d$	$\delta F_i^0$	$\delta F_j^1$	$\delta B_i^0$	$\delta B_j^1$	$\delta(F_d^0, F_d^1)$	$\delta(F_d^1, B_0^1)$	$\delta(B_d^0, B_d^1)$
$0 \equiv d \pmod{2}$	2	1	2	1	2	4	1
$1 \equiv d \pmod{2}$	2	1	2	1	2	1	1

## G A Gallery of Pipeline Parallel Schedules and Their Building Blocks

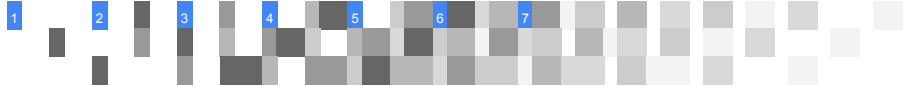
We show the building blocks and full schedules of some well-known existing methods in Figure 18.

## H Non-uniform Repeating Interval of Interleaved 1F1B

While most existing schedule in Figure 18 is repeated with uniform interval, Interleaved 1F1B [Narayanan et al., 2021] is slightly different in the repeating pattern. In Figure 15 we show two different repeating intervals. Official Interleaved 1F1B has a repeating interval as shown in Figure 15a. If we modify the repeating interval to Figure 15b, we’ll obtain another schedule with the same memory and bubble rate as official Interleaved 1F1B, shown in the gallery 18i.



(a) The Non-uniform repeating interval of Interleaved 1F1B. The number in highlighted grids shows the minibatch with that index starts at this cell



(b) A variation of Interleaved 1F1B with uniform repeat.

Figure 15: Different Repeat Pattern of The Same Building Block of Interleaved 1F1B.

## I Other Memory Efficient Building Blocks

Under the guidance of lifespan defined in 2.2, we can also find some of other building blocks besides the V-Shape building block family. We show the building blocks in Figure 16 and their full schedule in Figure 17. Both these schedules have lower bubble rate than 1F1B.

Specifically, 1F1B-V applies V-Shape to the building block of 1F1B but without *B-W* split, which can reduce the peak memory to asymptotically 2/3 of 1F1B.

We also find that utilizing *B-W* split, the zero bubble pipeline schedules proposed in [Qi et al., 2023] with configurable memory limit can support a minimum of 2/3 activation memory of 1F1B, using the building block shown in Figure 16b. Note that two microbatches are included in a single building block to avoid collision.

Using the building block defined in Figure 16c, we can have a schedule Figure 17c with the same bubble rate as Interleaved 1F1B but lower memory.

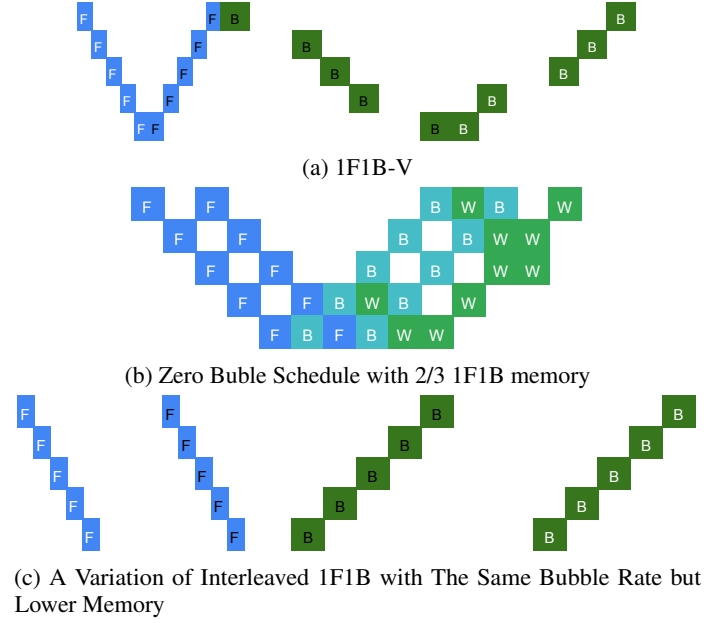


Figure 16: Other Memory-efficient Building Blocks.

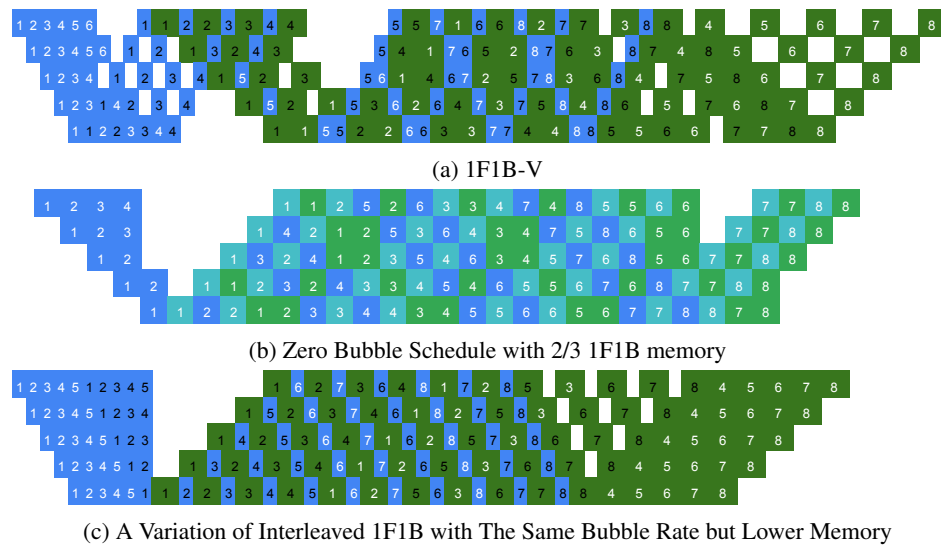


Figure 17: Other Memory-efficient Schedules.

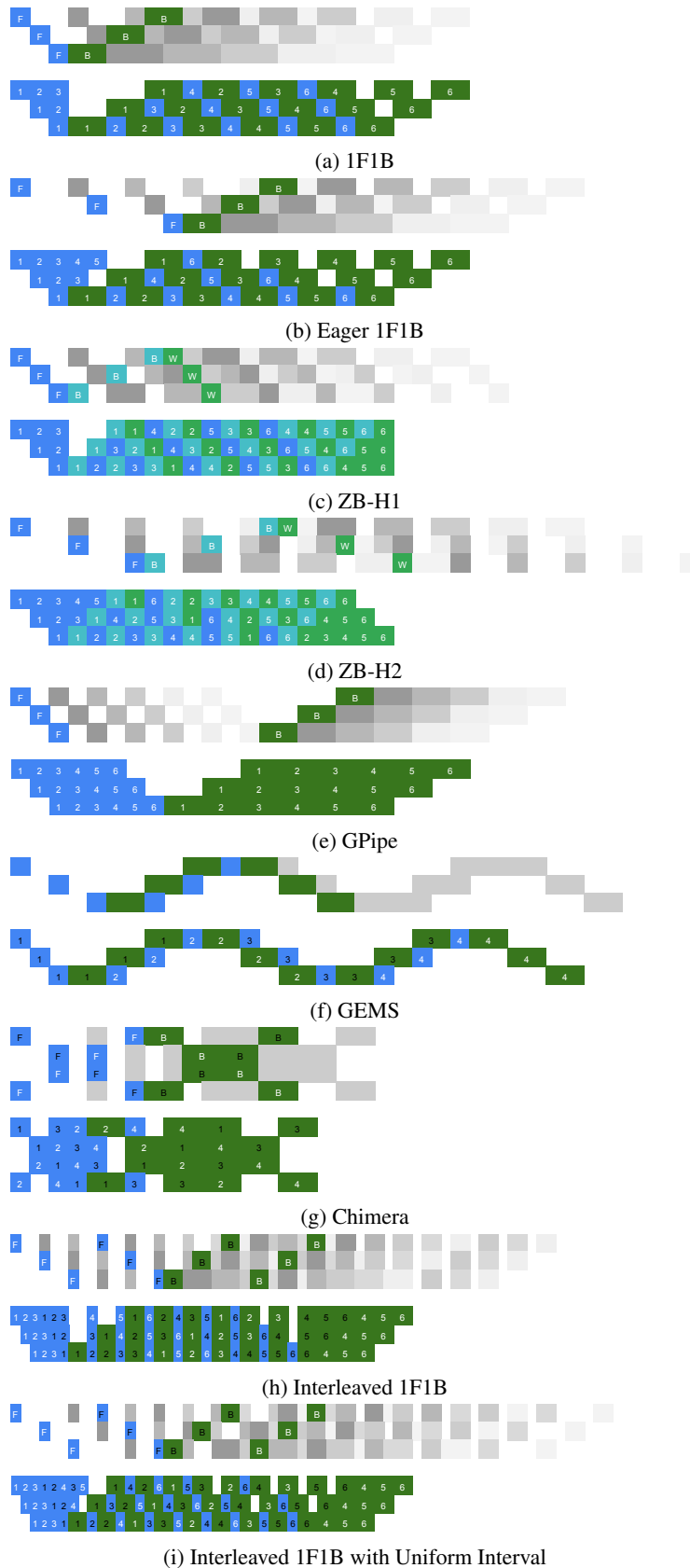


Figure 18: A Gallery of Pipeline Schedules and Their Building Blocks. The upper row of each schedule shows the building block and how it repeats. The lower row shows the final schedule after squeezing and reordering.